

Research Article

Silver Doped TiO₂ Nanostructure Composite Photocatalyst Film Synthesized by Sol-Gel Spin and Dip Coating Technique on Glass

Mojtaba Nasr-Esfahani¹ and Mohammad Hossein Habibi²

¹ Department of Materials Science and Engineering, Islamic Azad University, Najafabad Branch, Najafabad 85141-43131, Iran

² Department of Chemistry, University of Isfahan, Isfahan 81746-73441, Iran

Correspondence should be addressed to Mohammad Hossein Habibi, mhhhabibi@yahoo.com

Received 26 August 2007; Revised 9 January 2008; Accepted 20 February 2008

Recommended by Leonardo Palmisano

New composite films (P25SGF-MC-Ag, MPC500SGF-MC-Ag, and ANPSGF-MC-Ag) have been synthesized by a modified sol-gel method using different particle sizes of TiO₂ powder and silver addition. Nanostructure TiO₂/Ag composite thin films were prepared by a sol-gel spin and dip coating technique, while, by introducing methyl cellulose (MC) porous, TiO₂/Ag films were obtained after calcining at a temperature of 500°C. The as-prepared TiO₂ and TiO₂/Ag films were characterized by X-ray diffractometry, and scanning electron microscopy to reveal the structural and morphological differences. In addition, the photocatalytic properties of these films were investigated by degrading methyl orange (MO) under UV irradiation. After 500°C calcination, the microstructure of MC-TiO₂ film without Ag addition exhibited a microstructure, while significant sintering effect was noticed with Ag additions and the films exhibited a porous microstructure. Nanostructure anatase-phase TiO₂ can be observed with respect to the sharpening of XRD diffraction peaks. The photodegradation of porous TiO₂ deposited with 5×10^{-4} mol Ag exhibited the best photocatalytic efficiency, where 69% methyl orange can be decomposed after UV exposure for 1 hour.

Copyright © 2008 M. Nasr-Esfahani and M. H. Habibi. This is an open access article distributed under the Creative Commons Attribution License, which permits unrestricted use, distribution, and reproduction in any medium, provided the original work is properly cited.

1. INTRODUCTION

Titanium dioxide has attracted significant attention of researchers because of many interesting physical properties that make it suitable for a variety of applications, and TiO₂ has high corrosion resistance, chemical stability, and an excellent optical transparency in the visible and near infrared regions as well as high refractive index that makes it useful for antireflection coatings in optical devices. Efforts are devoted to the development of efficient water and air purification technologies, based on TiO₂ photocatalysis. Such a treatment typically reduces toxic organic compounds to nontoxic inorganic compounds, such as carbon dioxide, water, ammonium or nitrates, and chloride ions. A number of techniques, such as spray pyrolysis [1], sol-gel method [2], sputtering [3, 4], solvothermal method [5], pulsed laser deposition [6], atomic layer deposition [7], chemical vapour deposition (CVD) [8–12] and photoassisted CVD [13] have been used to deposit TiO₂ thin films. Each of the

techniques for the TiO₂ thin film preparation has its own advantages and disadvantages, and it remains unclear at present as to which of these will eventually prove to be the most cost/quality effective. The photocatalytic activity depends strongly on the surface redox potential and the lifetime of the photogenerated electron-hole pairs. Titanium dioxide exists in three different crystalline phases: anatase, rutile, and brookite. Anatase was found to be more active photocatalytically than rutile. This enhanced photoactivity is attributed to the larger bandgap existing in this crystalline phase, which generally leads to an increase of both the surface redox potential and the charge carrier lifetime. Due to the large surface area, thin and composite coatings consisting of anatase TiO₂ nanoparticles show high photocatalytic efficiency. The photocatalytic activity of TiO₂ coatings do not depend only on the phase, but also on the crystallite size and porosity [14]. Sol-gel derived titanium dioxide composites have been also developed and investigated for the purpose of producing thin and composite films and self-supported

photocatalysts. The resulting photocatalysts exhibit relatively high surface area and enhanced mechanical stability and integrity [15].

It is well known that the initiation step of the photocatalytic process consists in the generation of electron-hole pairs upon irradiation of the material with a photon having energy at least equal to that of the bandgap of the photocatalyst. The electron-hole pairs formed can either recombine in the bulk or travel up to the surface, where they can participate in chemical reaction involving species adsorbed on the external titanol groups. The only drawback of TiO_2 is that its band gap lies in the near-UV of the electromagnetic spectrum: 3.2 eV (388 nm) and 3.0 eV (410 nm) for anatase and rutile, respectively. As a consequence, only UV light is able to create electron-hole pairs and to initiate the photocatalytic processes. It is, therefore, evident that any modification of the TiO_2 -based photocatalysts, resulting in a lowering of its bandgap [16], is representing a breakthrough in the field. This is the reason why so many scientific works have appeared during recent years. An exhaustive analysis of the different approaches used to dope TiO_2 is beyond scope of this contribution and only a selection of cases will be summarized below. (i) One case is doping TiO_2 with various transition metals such as Au, Ag, Pt, Cr, Nb, V, Mn, and Fe [17, 18]. These systems show an enhanced photoactivity in the visible with an efficiency depending highly on the preparation method. However, they are characterized by thermal instability and by a critical control of the cluster dimension and distribution [19]. (ii) Another case is represented by TiO_2 doped with nonmetal atoms such as N, S, F, C, I, Br, and Cl [20, 21]. Also in this case, the photocatalytic activity depends on the content of nonmetal atoms and on the method of preparation. (iii) A third case is a dye-sensitized TiO_2 obtained by anchoring a dye on the surface of the photocatalyst [22]. Various dyes (catechol, porphyrins, phthalocyanines, etc.) have been employed as sensitizers, but most of them are toxic and, more important, easily undergo a self-degradation process, that makes them unsuitable for durable applications in photocatalysis. (iv) As a fourth case TiO_2 doped with silver particles must be mentioned. Electrons in the valence band of TiO_2 are excited to the conduction band, with formation of holes in the valence band. At the same time electrons of Ag nanoparticles, when irradiated with the light of their plasmon resonance wavelength, are excited and transformed to adsorbed oxygen with formation of O^{2-} . The Ag nanoparticles are consequently oxidized by O^{2-} to colorless Ag^+ ions [23, 24]. In presence of TiO_2 these Ag^+ ions are reduced by the excited electrons and Ag nanoparticles are reformed. A limiting factor of the photocatalytic reaction is, therefore, recombination of the electron and hole prior to the superoxide activation step [25]. Silver has been shown to have a beneficial influence on the photoactivity of nanocrystalline semiconductor photocatalysts [26–28]. The combination of semiconductor substrate and metal cluster has been reported to give improved photocatalytic activity by trapping the photoinduced charge carriers, thereby improving the charge transfer processes [29–32].

In our previous work [33], we described a simple and repeatable approach to achieve useful materials for photocatalytic application by direct mixing of dispersed nanopowder titanium dioxide in sol-gel solution with prepolymerized material (polymer). The polymer was introduced into the sol-gel precursors in order to prevent particle aggregation, adjust the viscosity of sol, increase the strength of the unfired materials, and prevent film crack formation. In this case, it is important to avoid phase separation throughout the sol-gel reaction by a careful choice of solvents and optimized material processing conditions. Methyl cellulose (MC) is one of the ideal prepolymerized materials due to its solubility in water, which is suitable for use in sol-gel processing. Another advantage is that MC belongs to nonionic cellulose ether, which is substantially free of substances that can induce crystallization of silica or titania, and so forth during any of the coating formation and densification process steps.

For the reasons briefly mentioned above, we became interested in modifying the light absorbing property and photocatalytic activity of nanostructure composite TiO_2 films covering glass slide. Coming now to this study, it can be divided into two parts. In the first part, we illustrate a new strategy to synthesize a silver-doped titanium dioxide characterized by the presence of large surface area. In the second part, we demonstrate that the layer consists of anatase, which is efficient to remove the adsorbed molecular species from the environment via photocatalytic reaction. In this study, we have successfully synthesized three types of composite films (P25SGF-MC-Ag, MPC500SGF-MC-Ag, and ANPSGF-MC-Ag) by a modified sol-gel method using different particle size of TiO_2 powder. Methyl cellulose (MC) was added as a template to the sol for stress reduction which improved the amount of crystalline material immobilized on the support and the grain size of the films calcined at 500°C. The as-deposited TiO_2/Ag films were characterized by X-ray diffractometry, scanning electron microscopy, differential scanning calorimetry, and thermal gravimetric analysis. In addition, photocatalytic properties of these films were evaluated by degrading methyl orange under UV irradiation. The purpose of this study is to obtain insights on how the incorporation of Ag into the modified titania composite films affects the photocatalytic activity of such macroporous films, so as to design high performance TiO_2 composite films for water treatment.

2. EXPERIMENTAL

Standard ethanol solution ($M = 46.07 \text{ g/mol}$, purity $\approx 99.8\%$) was purchased from Fluka Chemical. Hydrochloric acid ($M = 36.5 \text{ g/mol}$, purity $\approx 35.5\%$) and silver nitrate (99%) were supplied from Merck. Titanium tetra isopropoxide ($\text{Ti}(\text{iOPr})_4$ or TTIP) (Sigma-Aldrich, 97%), the precursor, was used without further purification. Three types of commercial TiO_2 powders, namely, Aldrich TiO_2 powder (ANP), Degussa P-25 (P25), and Millennium PC-500 (MPC500) were used as the filler in the nanostructure composite films. Specifications of the photocatalysts filler according to the manufacturer's data are given in Table 1. Methyl cellulose (low substitution) was used as an organic binder material

TABLE 1: Properties of TiO₂ nanopowders.

Photocatalyst	Composition	Specific BET surface area (m ² g ⁻¹)	Primary particle size (nm)
Aldrich powder TiO ₂ (ANP)	≥97% anatase	190–290	15
Millennium PC-500 (MPC500)	≥97% anatase	>250	5–10
Degussa P25 (P25)	70% anatase	~50	20

[24]. Methyl orange (4-[[4-dimethylamino]phenyl]azo) benzenesulfonic acid sodium salt) analytical grade [34] was chosen as a simple model of a series of common azo dyes largely used in the industry. Methyl orange is a well-known acid-base indicator, orange in basic medium, and red in acidic medium. The preparation steps for the composite films derived from TiO₂ powder are described in detail elsewhere [35]. The sol was prepared by adding 5 mL TTIP to a 50 mL beaker containing a mixture of 10 mL ethanol and 1.8 mL HCl 35.5% that had been mixed for five minutes. Methyl cellulose 2 wt.% solution was prepared using MC and double-distilled water. These two solutions (titanium precursor and MC solution) were added dropwise and stirred overnight at room temperature. Precalcinated TiO₂ nanopowders (ANP, P25, MPC500), Degussa P25 (P25), and Millennium PC-500 (MPC500) were used as filler mixed with the sol (5% of sol). TiO₂ powder was dispersed in the sol and the prepared mixtures were deposited on the microscope glass slide (75 mm × 25 mm × 1 mm) by homemade spin coating. The dried films were heated in a muffle furnace to 500°C at a heating rate 5°C min⁻¹ and maintained at this temperature for 60 minutes and cooled at room temperature with similar rate. Three different composite (P25SGF-MC, MPC500SGF-MC, and ANPSGF-MC) films were dipped into the silver nitrate solution with various molar concentrations (5×10^{-6} , 10^{-5} , 5×10^{-5} , 10^{-4} , 5×10^{-4} , 5×10^{-3} , 10^{-3} , 10^{-2} M) for three seconds, washed with distilled water, dried at nitrogen atmosphere and no color change was observed. The silver-doped composite films (P25SGF-MC-Ag, MPC500SGF-MC-Ag, and ANPSGF-MC-Ag) were irradiated with two UV-C lamps (8 W) for 2 hours in air and color change was observed. These composite films were used for photocatalytic degradation; otherwise the photocatalysts were stored in the dark to avoid preactivation by room light or sunlight.

Film morphology was characterized by an environmental scanning electron microscope (ESEM, JEOL JSM-5300LV) with accelerating 10 kV. The phase composition of photocatalyst was studied by the powder and plate XRD technique. The X-ray diffraction patterns were obtained on a D8 Advanced Bruker X-ray diffractometer using Cu K α radiation at an angle of 2θ from 15 to 60°. The scan speed was 1°/min. The strongest peaks of TiO₂ corresponding to anatase (1 0 1) and rutile (1 1 0) were selected to evaluate the crystallinity of the samples. The mean crystallite size L was determined from the broadening β of the most intense line, for each polymorph, in the X-ray diffraction pattern, based on the Scherrer equation:

$$L = \frac{k\lambda}{\beta \cos\theta}, \quad (1)$$

where λ is the radiation wavelength, $k = 0.90$, and θ is the Bragg angle [36].

Evaluation of the adhesion and bonding strength between the coating and glass substrate was made by using the scratch test technique.

The photocatalytic activity of films was evaluated by degrading methyl orange solution. The distance between the UV light source and deposited films was set as 10 cm. Sol-gel derived films were prepared on microscopy glass slides. To evaluate the catalytic activity, the photodegradation of methyl orange solution was chosen as a simple model of a series of common azo dyes largely used in the industry. One TiO₂-Ag/glass with one time spin coating (75 mm × 25 mm × 1 mm) was used as photocatalyst and irradiated with two 8 W UV-A ($\lambda = 365$ nm) at a distance of 5 cm from the top of the solutions. 20 mL of the dye solutions with initial concentration of 5 ppm at pH = 4.5 was used. The solution was stirred in the dark for 90 minutes before irradiation to reach an equilibrated adsorption. Therefore, this time has been selected for the initial period to UV-irradiation to make sure that the initial degradation initiates at the equilibrium of the adsorption. The color removal of the dye solution was followed by measuring the absorbance value at $\lambda = 460$ nm, using double beam UV-visible spectrophotometer, (Varian Cary 500 Scan) initially calibrated, according to Beer-Lambert's law.

3. RESULTS AND DISCUSSION

Sol-gel derived composite film [25] can be easily employed as a fast and nonenergy consuming procedure to mass production of titania composite films (of 10 μ m in thickness) with good uniformity and reproducible properties. After dipping of the TiO₂ composite films in the silver nitrate solution and subsequent UV irradiation at 254 nm for 2 hours, the photocatalyst appears dark brown. Increasing the Ag⁺ concentration of dipping solution produces darker films at a gradient rate. Macroscopic observation of the film suggests that silver particles are widely spread on the surface without the formation of islands and that the resulting surface modified photocatalysts possess a solid structure on the glass substrate with more than satisfactory scratch resistance and adherence.

An XRD pattern of sol-gel derived TiO₂ thin film heat treated at 500°C for 1 hour shows that anatase was formed without contamination by other polymorphs: brookite or rutile (Figure 1). Nonheated thin film had an amorphous (and/or an ultra-fine crystalline) structure with a very broad peak at about $2\theta = 25^\circ$ (which is identified as the most intensive peak (1 0 1) for the anatase TiO₂). Diffraction peaks of anatase were observed for the coatings heat treated at

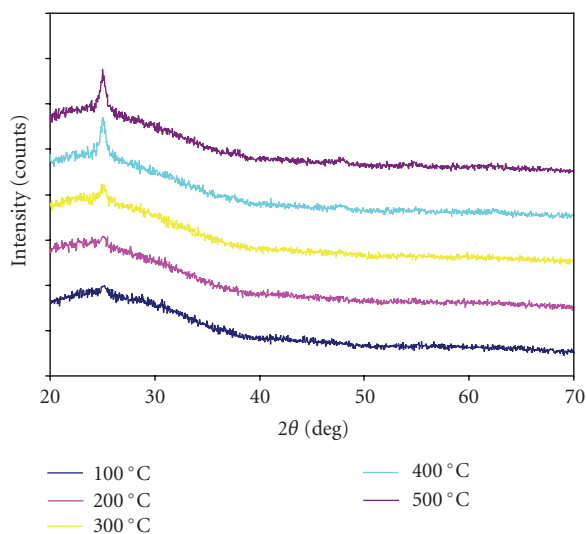


FIGURE 1: XRD patterns of TiO_2 sol-gel derived thin film by one time spin coating with heat treated at different temperatures.

temperatures higher than 300°C . Diffraction peaks of rutile were not found for the gel-derived deposited coatings heated up to 500°C .

The XRD patterns of different composite sol-gel samples (P25SGF-MC, ANPSGF-MC, and MPC500SGF-MC) before and after Ag coating are shown in Figure 2. As shown in Figure 2(a), for P25SGF-MC anatase/rutile ratio remains almost constant, as compared with the filler phase composition, after heating up to 500°C . This is because of the relatively high percentage of TiO_2 amount (the filler) compared to the amount of TiO_2 which is derived from the sol. For ANPSGF-MC and MPC500SGF-MC nanostructure composite films, which are prepared by ANP and MPC500 nanopowder, since ANP and MPC500 contain 100% anatase, diffraction peaks of rutile were not found (Figures 2(b) and 2(c)).

It can be found that films exhibited the TiO_2 composite films calcined at 500°C show relative sharp peaks indicating the coalescence of nanocrystalline anatase-phase TiO_2 . According to the Figures 2(a), 2(b), and 2(c), the intensity of the anatase and rutile main peaks in the nanostructure composite films, both before coating or after coating by Ag, are very similar. It is noticed that no additional XRD peaks corresponding to Ag additions can be revealed. This may be attributed to the well dispersion of nanocrystalline Ag particles in the TiO_2 matrix, the overlapping of Ag XRD peak or silver oxide particles are not crystallized on TiO_2 surface. On the contrary, well-organized crystal structure from titania particles is observed for the all composite films.

As shown in Table 2, for the sample sol-gel dried gel modified with MC, the crystallite size of anatase phase, which was used as a measure of TiO_2 crystallinity, increases considerably with calcinations temperature, from about 0.5 nm at room temperature to 13.4 nm at 500°C . However, for P25 and ANP, the initial anatase crystallite size increased only slightly versus temperature, from 15 nm for anatase

at room temperature to more than 16.3 nm for anatase, in ANP (at 500°C) and more than 19.2 nm for anatase, in P25 powder (at 500°C). It is suggested that the growth process of nanocrystalline anatase is mainly because of the sintering of the single crystals within the agglomerates, and finally the original agglomerate transforms to a larger single crystal [37]. However, as shown in Table 2, For MPC500 nanopowder is observed that the initial anatase crystallite size increased more significantly versus temperature, comparing other nanopowder TiO_2 .

For the heat-treated sol-gel derived composite film, the crystallite size is mainly determined by the particle size of the calcined filler powder and remains approximately constant up to 500°C . The average size of the grains in TiO_2 films prepared by P25, ANP, and MPC500 in the sol was approximately 18.6, 16.3, and 18.1 nm, respectively. The grain size of composite films, prepared with ANP which is 16.3 nm, is only a little larger than the average crystal size of ANP particles (15 nm), which demonstrates that ANP particles in the sol under these conditions cannot form much larger grains. The grain size of composite film prepared by MPC500 particles in the sol is much larger than the average crystal size of MPC500 particles (5–10 nm), which indicates that MPC500 particles in the sol can aggregate to form larger grains. It is worth to mention that the composite film with MPC500 has more scratch adhesion than other one which is confirmed by XRD and SEM images.

Because the decomposition temperature of MC as template is below 400°C , porous TiO_2 composite films can be prepared by calcining at 500°C to remove the MC microspheres. However, conventional SEM (Figure 3(a)) can only reveal a smooth surface of TiO_2 films made from the precursor sol containing no nanopowder heat treated for 1 hour at 500°C and no individual TiO_2 grain can be observed. Figure 3(b) shows the high-magnification field-emission ESEM micrograph ANPSGF-MC and Figure 3(c) shows MPC500SGF-MC after calcining where nanocrystalline TiO_2 particles can be observed. As shown in Figures 3(b) and 3(c), the diameter of the calcined TiO_2 nanoparticles was small (less than 20 nm).

In order to check the adhesion strength of these photocatalytic films on the glass substrate, scratch test technique is performed on these films. All composite films calcined at 500°C and the results are provided in Table 2, which demonstrates that 500°C is the optimum calcination temperature at or above which excellent adhesion between the nanostructure composite films and the glass substrate can be obtained. For P25, ANP, and MPC500 TiO_2 nanopowder coatings deposited from slurry (i.e., without the sol binder), the normal load needed to remove the coatings from the substrate is $\sim 0 \text{ g/mm}^2$. In fact, this load is so small that can be considered as zero, especially when compared to the respective values for the nanostructure composite films, in the range of 200–350 gr/mm^2 .

The photocatalysis experiments took place in an aqueous solution of methyl orange to evaluate the composite films activity. The photocatalytic activity was evaluated as the percentage of pollutant disappearance. The photodegradation of methyl orange was followed using absorption at λ_{max} 270 nm

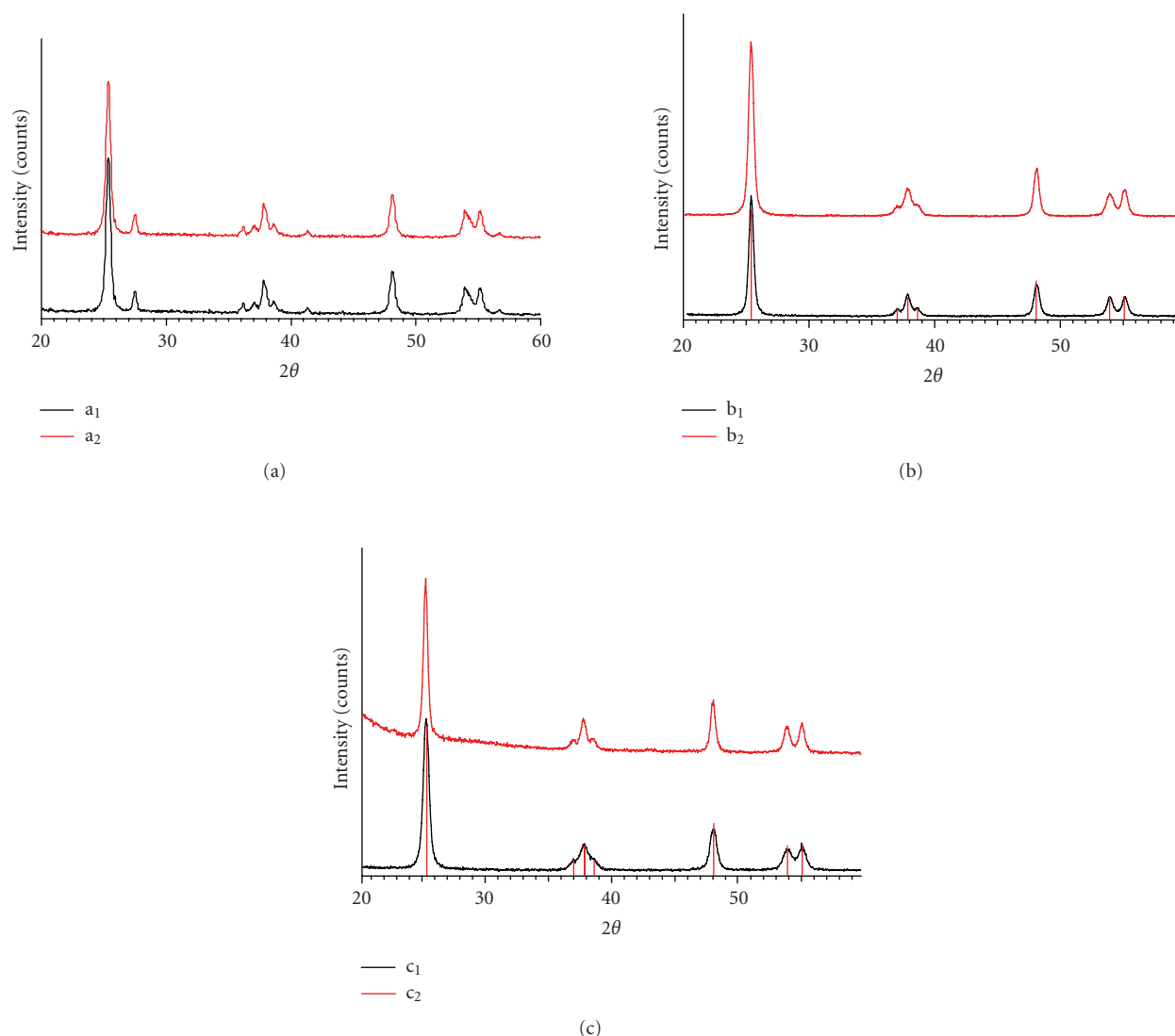


FIGURE 2: (a) XRD patterns of (a₁) sol-gel derived composite film from Degussa P25 TiO₂ with MC heat treated for 1 hour at 500°C (P25SGF-MC) and (a₂) after silver deposition (P25SGF-MC-Ag). (b) X-ray diffraction patterns of (b₁) sol-gel derived composite film from Mellenium PC 500 TiO₂ with MC heat treated for 1 hour at 500°C (MPC500SGF-MC) and (b₂) after silver deposition (MPC500SGF-MC-Ag). (c) X-ray diffraction patterns of (c₁) sol-gel derived composite film from Aldrich nanopowder TiO₂ with MC heat treated for 1 hour at 500°C (ANPSGF-MC) and (c₂) after silver deposition (ANPSGF-MC-Ag).

and 505 nm during the photodegradation reaction as a function of irradiation time. The color of methyl orange solution changes from orange to red and finally become colorless with increasing irradiation time. It should be pointed out that decomposition of methyl orange itself under UV irradiation is negligible. Each experimental set was repeated three times. The results were reproducible within narrow limits (2%) and the mean value was selected. Detailed preliminary tests were first performed in order to determine minor silver deposition parameters such as dipping duration and UV illumination time. The results with different AgNO₃ solutions have shown that the optimum conditions correspond to 3-second dipping and a 120-minute UV illumination, respectively, leading to silver-modified titania films with the best photocatalytic effect. It was also confirmed that the crucial parameter that

strongly influences the films photocatalytic activity is the concentration of the AgNO₃ dipping solution.

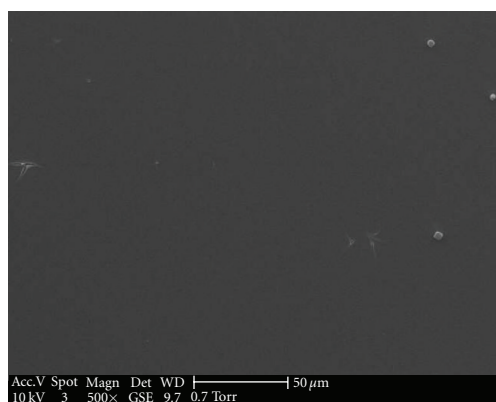
The photocatalytic efficiency (degradation percentage corresponding to 1-hour illumination) of the silver-doped titania nanostructure composite films for the MO decomposition are illustrated in Figures 4(a), 4(b), and 4(c). The corresponding performance of the original nonsupported nanostructure composite titania films is also given for comparison. The porous P25SGF-MC-Ag, MPC500SGF-MC-Ag, and ANPSGF-MC-Ag composite films exhibited 69%, 42%, and 64% degradation, respectively, after the same exposure time.

As shown in Figure 4(a), the results show that by increasing the concentration of the dipping solution, the photocatalytic efficiency of ANPSGF-MC increases. A maximum

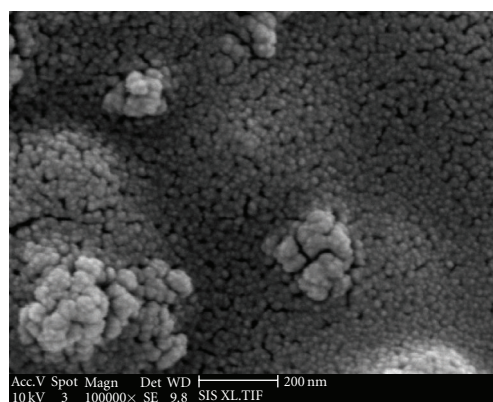
TABLE 2: Physical and chemical characteristics of different TiO₂ photocatalysts.

Material	Heat-treatment conditions	Particle size (nm) ^(a)	Scratch adhesion (g/mm ²)
Sol-gel derived TiO ₂	—	—	150
modified with MC	500°C, 1 h	13.4	1500
P25	—	18.8	~0
	500°C, 1 h	19.2	~0
ANP	—	15	~0
	500°C, 1 h	16.3	~0
MPC500	—	6.6	~0
	500°C, 1 h	16.7	~0
ANPSGF-MC	—	14.9	9
	500°C, 1 h	16.3	200
MPC500SGF-MC	—	6.6	10
	500°C, 1 h	18.1	350
P25SGF-MC	—	19.2	10
	500°C, 1 h	18.6	200

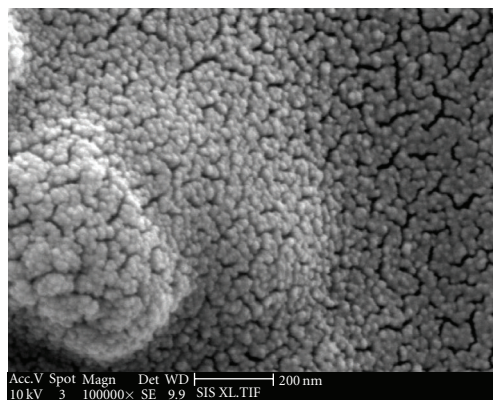
^(a) Using Scherrer equation: $D = 0.9\lambda / (B \cos \theta)$, where $\lambda = 0.15418$ nm.



(a)



(b)



(c)

FIGURE 3: Scanning electron micrographs of the surface of TiO₂ films made from the precursor sol containing (a) no nanopowder, (b) ANPSGF-MC-Ag, and (c) MPC500SGF-MC-Ag. All the samples are heat treated for 1 hour at 500°C.

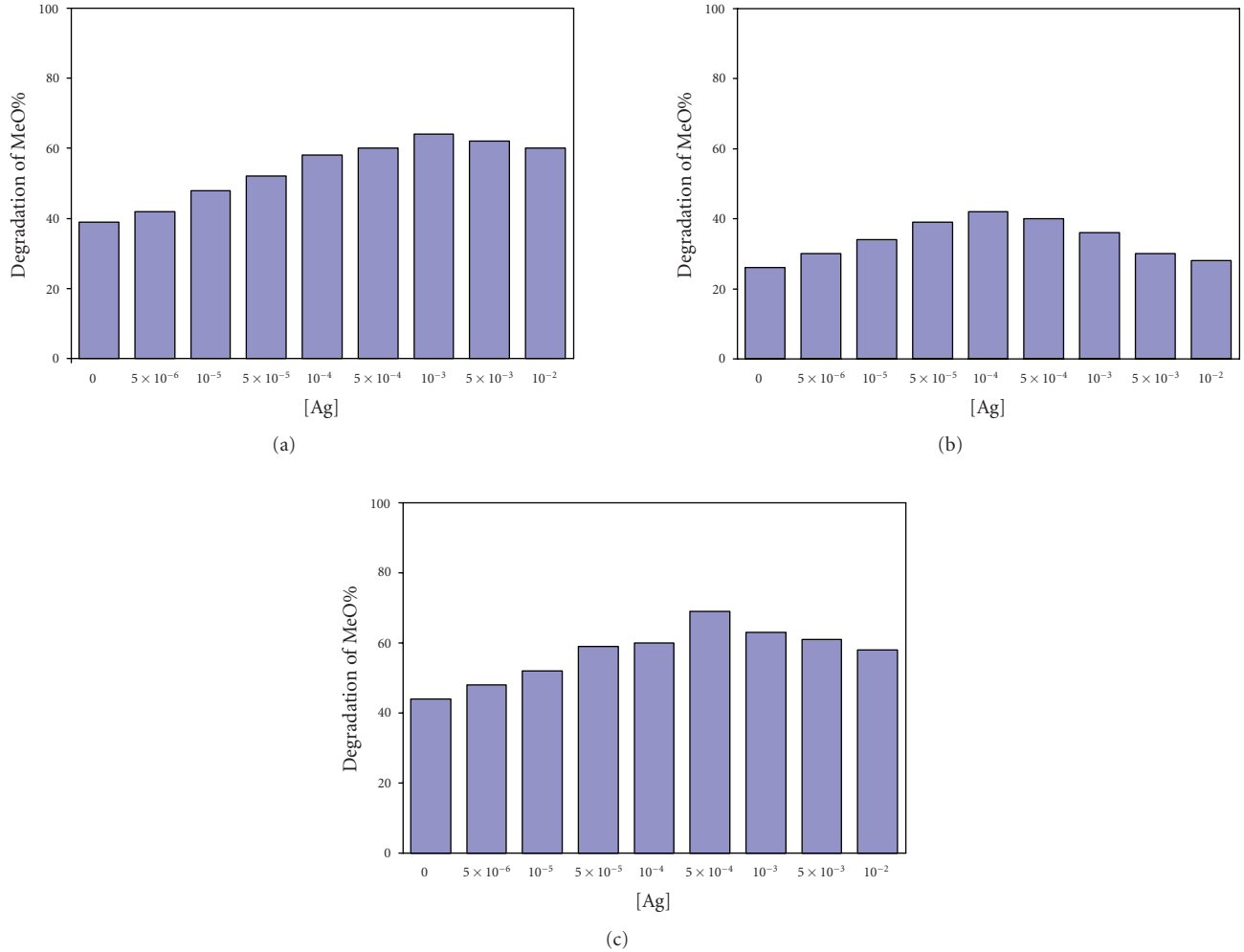


FIGURE 4: Effect of the Ag loading in the composite films on the photocatalytic activity, (a) ANPSGF-MC-Ag, (b) MPC500SGF-MC-Ag, and (c) P25SGF-MC-Ag. Conditions of the photocatalytic experiments: one-time spin coating ($75 \text{ mm} \times 25 \text{ mm} \times 1 \text{ mm}$) was used as photocatalyst and irradiated with two 8 W UV-A ($\lambda = 365 \text{ nm}$) at a distance of 5 cm from the top of the solutions. 20 mL of the dye solutions with initial concentration of 5 mg/L at pH = 4.5.

(64%) is observed for ANPSGF-MC-Ag films immersed in 10^{-3} M AgNO_3 solution. Further increase of the Ag^+ concentration results in a considerable efficiency decrease. For instance, for ANPSGF-MC films dipped in 10^{-2} M AgNO_3 solution the MO decomposition percentage goes to 58%. More spectacularly, it falls to lower decomposition percentage for more concentrated AgNO_3 , a value lower than that obtained with the nonsupported composite film. It is suspected that superfluous Ag additions reduced the surface activation sites of TiO_2 and thus the degradation efficiency decreased.

As shown in Figures 4(b) and 4(c), the similar results are obtained for other nanostructure composite films (MPC500SGF-MC-Ag and P25SGF-MC-Ag). A maximum (42%) is observed for the MPC500SGF-MC-Ag films immersed in 10^{-4} M AgNO_3 solution, while for P25SGF-MC-Ag films, maximum degradation percentage (69%) is observed after immersion in 5×10^{-4} M AgNO_3 solution. It is interesting to note that the composite film with P25 has more

photo efficiency than other one, however photoefficiency of ANPSGF-MC after coating by Ag have promoted more than other one comparing to the pure titania films. According to the results, ANPSGF-MC composite films have more ability to dope with Ag particles comparing other composite films (P25SGF-MC and MPC500SGF-MC), which is confirmed by difference in grain size of TiO_2 in these composite films.

Sol-gel derived porous and nanostructure composite film prepared by P25 (P25SGF-MC) after coating with Ag exhibited the best photocatalytic performance. It has been reported that porous TiO_2 films [4] or Ag-doped TiO_2 films [13] show an enhanced photocatalytic efficiency. In the present study, we have demonstrated the improved photocatalytic performance with both porous structure and Ag additions. Practical applications of these films are highly potential.

Figures 5(a), 5(b), and 5(c) show the photodegradation results of the TiO_2 nanostructure composite films, after deducting both the self-degradation of methyl orange under

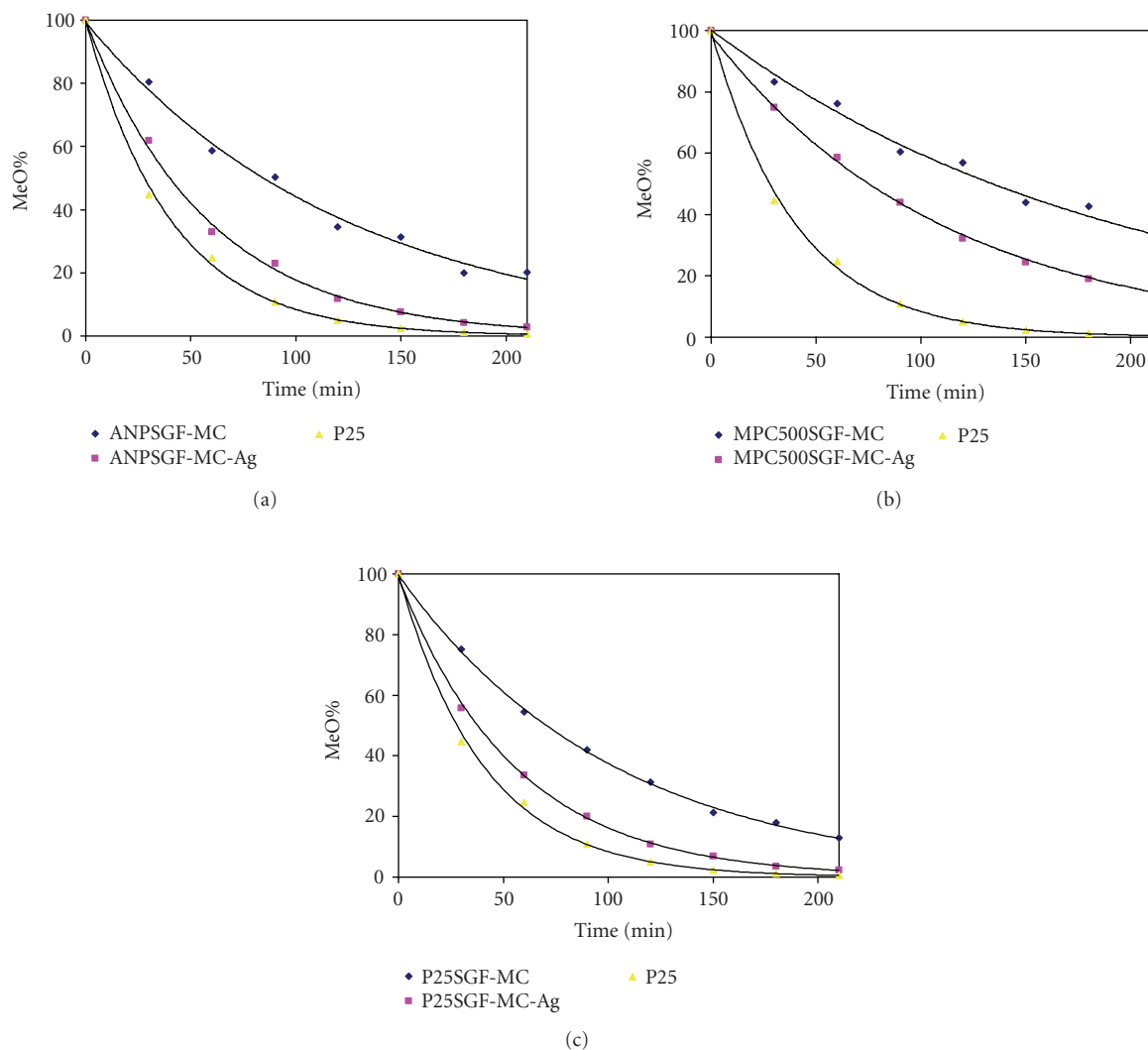


FIGURE 5: (a) Plot of the percent of MO remaining after photodegradation versus irradiation time in the presence of (a) \blacklozenge ANPSGF-MC composite film, (b) \blacksquare ANPSGF-MC-Ag composite film (immersed in 10^{-3} M AgNO_3 solution), and (c) \blacktriangle TiO_2 suspension. Conditions of the photocatalytic experiments: one-time spin coating ($75 \text{ mm} \times 25 \text{ mm} \times 1 \text{ mm}$) was used as photocatalyst and irradiated with two 8 W UV-A ($\lambda = 365 \text{ nm}$) at a distance of 5 cm from the top of the solutions. 20 mL of the dye solutions with initial concentration of 5 mg/L at pH = 4.5. (b) Plot of the percent of MO remaining after photodegradation versus irradiation time in the presence of (a) \blacklozenge MPC500SGF-MC composite film, (b) \blacksquare MPC500SGF-MC-Ag composite film (immersed in 10^{-3} M AgNO_3 solution), and (c) \blacktriangle TiO_2 suspension. Conditions of the photocatalytic experiments: one-time spin coating ($75 \text{ mm} \times 25 \text{ mm} \times 1 \text{ mm}$) was used as photocatalyst and irradiated with two 8 W UV-A ($\lambda = 365 \text{ nm}$) at a distance of 5 cm from the top of the solutions. 20 mL of the dye solutions with initial concentration of 5 mg/L at pH = 4.5. (c) Plot of the percent of MO remaining after photodegradation versus irradiation time in the presence of (a) \blacklozenge P25SGF-MC composite film, (b) \blacksquare P25SGF-MC-Ag composite film (immersed in 10^{-3} M AgNO_3 solution), and (c) \blacktriangle TiO_2 suspension. Conditions of the photocatalytic experiments: one-time spin coating ($75 \text{ mm} \times 25 \text{ mm} \times 1 \text{ mm}$) was used as photocatalyst and irradiated with two 8 W UV-A ($\lambda = 365 \text{ nm}$) at a distance of 5 cm from the top of the solutions. 20 mL of the dye solutions with initial concentration of 5 mg/L at pH = 4.5.

UV and physical adsorption. Methyl orange photodegradation kinetics permitted to directly compare the performance of the silver-modified photocatalysts to the nonsupported materials. It is clear that under the experimental conditions used, all photocatalytic curves follow first-order reaction kinetics. Initial reaction conditions provide realistic comparison of the photodegradation rates. To a reasonable approximation, the slope of the fitted lines corresponds to a relative pseudo-first-order rate constant [28]. Kinetic

parameters after 2 hours of illumination for decolorization of MO are summarized in Table 3.

It is obvious that all nanostructure composite TiO_2 films after coating by Ag are more efficient catalysts, comparing to the pure titania film. This can be explained on the basis of surface characteristics. Complete pollutant decolorization for P25SGF-MC-Ag was achieved after 120 minutes of illumination and for P25SGF-MC film after about 240 minutes, respectively. As shown in Figures 4(a) and 4(b) and Table 3,

TABLE 3: The rate constant for degradation of MO for nanostructure composite films with different mol percentages of silver.

Concentration of AgNO ₃ dipping solution (M)	Rate constant (min ⁻¹)		
	ANPSGF-MC	MPC500SGF-MC	P25SGF-MC
0	0.0081	0.0052	0.0098
5×10^{-6}	0.0098	0.0062	0.0115
1×10^{-5}	0.0115	0.0069	0.0132
5×10^{-5}	0.0128	0.0081	0.0158
1×10^{-4}	0.0151	0.009	0.0161
5×10^{-4}	0.0162	0.0082	0.0181
1×10^{-3}	0.0173	0.0064	0.0163
5×10^{-3}	0.0166	0.0060	0.0158
1×10^{-2}	0.0153	0.0051	0.0143

the silver-modified composite film prepared by MPC500 (MPC500SGF-MC-Ag) showed lower photocatalytic activity than the film prepared by ANP (ANPSGF-MC-Ag). The impact of surface area on the photocatalytic activity is clearly demonstrated, where MPC500SGF-MC-Ag film shows significantly lower degradation rate than ANPSGF-MC-Ag. As a result, P25SGF-MC-Ag nanostructure composite films show more photoefficiency than other composite films, which was as expected due to presence of rutile phase in Degussa P-25 powder. We encapsulated Degussa P25 TiO₂ instead of preparing the films in order to have a combination of anatase and rutile phases in the TiO₂ films, since the presence of rutile phase enhances the activity of the anatase phase by serving as an electrons' sink. In fact, by encapsulating P25 TiO₂ within mesoporous TiO₂ film, it should be possible to optimize the two components of the composite film, for example, by incorporating more active TiO₂ particles [14]. In this work, it was found that an incorporation of commercial anatase nanoparticles into the TiO₂ thin films, then coating them by Ag provides advantages in the photodecomposition of TiO₂ by eliminating the filtration of the solutions, therefore, allowing for more efficient processes.

To evaluate the catalytic strength changes due to immobilization of the catalysts and compare the films efficiency to the Degussa P25 powder, the film weight was measured. The slurry concentration of TiO₂ was then adjusted to meet the exact quantity of TiO₂ nanostructure composite immobilized film, in order to safely compare the obtained results. Thus, a pollutant solution (20 mL) was also photolyzed in the presence of a suspension (dispersion) of Degussa P25 powder (0.0032 g = 160 ppm) and the results are represented in Figures 5(a), 5(b), and 5(c). The slope for the slurry is greater than that of the silver-modified nanostructure composite films, showing a higher efficiency as a photocatalyst. Complete depolarization of MO occurs in less than 90 minutes. It is worth mentioning that on composite film samples, only a part of the catalyst is exposed to the pollutant solution and it can, therefore, be photocatalytically active. As a result, a decrease in the overall photocatalytic performance of composite films compared to slurry solution is expected. This difference can be easily understood, if one considers that the photocatalytic process

is a surface and not a volume or mass phenomenon. The active photocatalyst is the illuminated TiO₂ material, which can be in contact with the organic pollutant. As Degussa's powder surface area is very high (50 m²g⁻¹), the slurry's surface is much higher than the film's real external surface and the silver synergetic action cannot promote such a high efficiency. However, the specific surface area of most of the composite samples, at the heat treatment (500°C), changes mostly due to the increase in the surface area of the sol-gel derived TiO₂ (titania sol), as a result of the decomposition and oxidation of the organic residues (i.e., MC), the evaporation of the solvent and excess water, and so forth.

4. CONCLUSION

In the present study, we have prepared nanostructure composite films developed on microscope glass slides by a sol-gel spin coating technique and were modified by silver deposition, characterized and successfully tested for the photocatalytic degradation of the pollutant methyl orange. TiO₂/Ag films were obtained by introducing MC microspheres and calcining at a temperature of 500°C. All the prepared composite films exhibited anatase-phase TiO₂ as determined by XRD. MC-TiO₂ films with Ag additions exhibited porous nanostructure but differed from that of porous TiO₂ film. The photocatalytic properties of the prepared thin films were evaluated by degrading methyl orange under UV. ANPSGF-MC-Ag, MPC500SGF-MC-Ag, and P25SGF-MC-Ag composite films exhibited 64%, 42%, and 69% degradation, respectively. By making the TiO₂ film porous and adding Ag element, the photocatalytic performance of the TiO₂-based composite films can be improved significantly.

ACKNOWLEDGMENTS

The authors wish to thank the Center of Excellency (Chemistry), University of Isfahan for financially supporting this work and Islamic Azad University, Najafabad Branch for their partial support.

REFERENCES

- [1] M. O. Abou-Helal and W. T. Seeber, "Preparation of TiO₂ thin films by spray pyrolysis to be used as a photocatalyst," *Applied Surface Science*, vol. 195, no. 1–4, pp. 53–62, 2002.
- [2] J. Yu, X. Zhao, and Q. Zhao, "Photocatalytic activity of nanometer TiO₂ thin films prepared by the sol-gel method," *Materials Chemistry and Physics*, vol. 69, no. 1–3, pp. 25–29, 2001.
- [3] S. K. Zheng, T. M. Wang, G. Xiang, and C. Wang, "Photocatalytic activity of nanostructured TiO₂ thin films prepared by dc magnetron sputtering method," *Vacuum*, vol. 62, no. 4, pp. 361–366, 2001.
- [4] D. Dumitriu, A. R. Bally, C. Ballif, et al., "Photocatalytic degradation of phenol by TiO₂ thin films prepared by sputtering," *Applied Catalysis B*, vol. 25, no. 2–3, pp. 83–92, 2000.
- [5] S.-H. Lee, M. Kang, S. M. Cho, et al., "Synthesis of TiO₂ photocatalyst thin film by solvothermal method with a small amount of water and its photocatalytic performance," *Journal of Photochemistry and Photobiology A*, vol. 146, no. 1–2, pp. 121–128, 2001.
- [6] R. Paily, A. DasGupta, N. DasGupta, et al., "Pulsed laser deposition of TiO₂ for MOS gate dielectric," *Applied Surface Science*, vol. 187, no. 3–4, pp. 297–304, 2002.
- [7] J. Aarik, A. Aidla, T. Uustare, et al., "Atomic layer deposition of TiO₂ thin films from TiL₄ and H₂O," *Applied Surface Science*, vol. 193, no. 1–4, pp. 277–286, 2002.
- [8] D. Byun, Y. Jin, B. Kim, J. K. Lee, and D. Park, "Photocatalytic TiO₂ deposition by chemical vapor deposition," *Journal of Hazardous Materials*, vol. 73, no. 2, pp. 199–206, 2000.
- [9] M. L. Hitchman and F. Tian, "Studies of TiO₂ thin films prepared by chemical vapour deposition for photocatalytic and photoelectrocatalytic degradation of 4-chlorophenol," *Journal of Electroanalytical Chemistry*, vol. 538–539, pp. 165–172, 2002.
- [10] A. Mills, N. Elliot, I. P. Parkin, S. A. O'Neill, and R. J. Clark, "Novel TiO₂ CVD films for semiconductor photocatalysis," *Journal of Photochemistry and Photobiology A*, vol. 151, no. 1–3, pp. 171–179, 2002.
- [11] V. G. Bessergenev, I. V. Khmelinskii, R. J. F. Pereira, V. V. Krisuk, A. E. Turgambaeva, and I. K. Igumenov, "Preparation of TiO₂ films by CVD method and its electrical, structural and optical properties," *Vacuum*, vol. 64, no. 3–4, pp. 275–279, 2002.
- [12] V. G. Bessergenev, R. J. F. Pereira, M. C. Mateus, I. V. Khmelinskii, E. Burkel, and R. C. Nicula, "TiO₂ thin film synthesis from complex precursors by CVD, its physical and photocatalytic properties," *International Journal of Photoenergy*, vol. 5, no. 2, pp. 99–105, 2003.
- [13] N. Kaliwot, J.-Y. Zhang, and I. W. Boyd, "Characterisation of TiO₂ deposited by photo-induced chemical vapour deposition," *Applied Surface Science*, vol. 186, no. 1–4, pp. 241–245, 2002.
- [14] Y. Djaoued, S. Badilescu, P. V. Ashrit, D. Bersani, P. P. Lottici, and R. Brüning, "Low temperature sol-gel preparation of nanocrystalline TiO₂ thin films," *Journal of Sol-Gel Science and Technology*, vol. 24, no. 3, pp. 247–254, 2002.
- [15] M. Keshmiri, M. Mohseni, and T. Troczynski, "Development of novel TiO₂ sol-gel-derived composite and its photocatalytic activities for trichloroethylene oxidation," *Applied Catalysis B*, vol. 53, no. 4, pp. 209–219, 2004.
- [16] R. Isono, T. Yoshimura, and K. Esumi, "Preparation of Au/TiO₂ nanocomposites and their catalytic activity for DPPH radical scavenging reaction," *Journal of Colloid and Interface Science*, vol. 288, no. 1, pp. 177–183, 2005.
- [17] S. Rodrigues, K. T. Ranjit, S. Uma, I. N. Martyanov, and K. J. Klabunde, "Single-step synthesis of a highly active visible-light photocatalyst for oxidation of a common indoor air pollutant: acetaldehyde," *Advanced Materials*, vol. 17, no. 20, pp. 2467–2471, 2005.
- [18] P. N. Kapoor, S. Uma, S. Rodriguez, and K. J. Klabunde, "Aerogel processing of MTi₂O₅ (M = Mg, Mn, Fe, Co, Zn, Sn) compositions using single source precursors: synthesis, characterization and photocatalytic behavior," *Journal of Molecular Catalysis A*, vol. 229, no. 1–2, pp. 145–150, 2005.
- [19] W. Choi, A. Termin, and M. R. Hoffmann, "The role of metal ion dopants in quantum-sized TiO₂: correlation between photoreactivity and charge carrier recombination dynamics," *Journal of Physical Chemistry*, vol. 98, no. 51, pp. 13669–13679, 1994.
- [20] S. Usseglio, A. Damin, D. Scarano, S. Bordiga, A. Zecchina, and C. Lamberti, "(I₂)_n encapsulation inside TiO₂: a way to tune photoactivity in the visible region," *Journal of the American Chemical Society*, vol. 129, no. 10, pp. 2822–2828, 2007.
- [21] H. Luo, T. Takata, Y. Lee, J. Zhao, K. Domen, and Y. Yan, "Photocatalytic activity enhancing for titanium dioxide by co-doping with bromine and chlorine," *Chemistry of Materials*, vol. 16, no. 5, pp. 846–849, 2004.
- [22] D. Chatterjee and S. Dasgupta, "Visible light induced photocatalytic degradation of organic pollutants," *Journal of Photochemistry and Photobiology C*, vol. 6, no. 2–3, pp. 186–205, 2005.
- [23] K. Naoi, Y. Ohko, and T. Tatsuma, "TiO₂ films loaded with silver nanoparticles: control of multicolor photochromic behavior," *Journal of the American Chemical Society*, vol. 126, no. 11, pp. 3664–3668, 2004.
- [24] W. Chen, J. Zhang, Q. Fang, et al., "Sol-gel preparation of thick titania coatings aided by organic binder materials," *Sensors and Actuators B*, vol. 100, no. 1–2, pp. 195–199, 2004.
- [25] H. Gerischer and A. Heller, "The role of oxygen in photooxidation of organic molecules on semiconductor particles," *Journal of Physical Chemistry*, vol. 95, no. 13, pp. 5261–5267, 1991.
- [26] C. A. K. Gouvêa, F. Wypych, S. G. Moraes, N. Durán, and P. Peralta-Zamora, "Semiconductor-assisted photodegradation of lignin, dye, and kraft effluent by Ag-doped ZnO," *Chemosphere*, vol. 40, no. 4, pp. 427–432, 2000.
- [27] M. J. Height, S. E. Pratsinis, O. Mekasuwandumrong, and P. Praserttham, "Ag-ZnO catalysts for UV-photodegradation of methylene blue," *Applied Catalysis B*, vol. 63, no. 3–4, pp. 305–312, 2006.
- [28] S. Chen and U. Nickel, "Controllable exciton bleaching and recovery observed in ZnO-Ag hybrid nanometre-sized particles," *Chemical Communications*, no. 2, pp. 133–134, 1996.
- [29] T. Abe, E. Suzuki, K. Nagoshi, K. Miyashita, and M. Kaneko, "Electron source in photoinduced hydrogen production on Pt-supported TiO₂ particles," *Journal of Physical Chemistry B*, vol. 103, no. 7, pp. 1119–1123, 1999.
- [30] V. Subramanian, E. E. Wolf, and P. V. Kamat, "Semiconductor-metal composite nanostructures. To what extent do metal nanoparticles improve the photocatalytic activity of TiO₂ films?" *Journal of Physical Chemistry B*, vol. 105, no. 46, pp. 11439–11446, 2001.
- [31] V. Subramanian, E. E. Wolf, and P. V. Kamat, "Green emission to probe photoinduced charging events in ZnO-Au nanoparticles. Charge distribution and Fermi-level equilibration,"

- Journal of Physical Chemistry B*, vol. 107, no. 30, pp. 7479–7485, 2003.
- [32] W. Y. Teoh, L. Mädler, D. Beydoun, S. E. Pratsinis, and R. Amal, “Direct (one-step) synthesis of TiO_2 and Pt/TiO_2 nanoparticles for photocatalytic mineralisation of sucrose,” *Chemical Engineering Science*, vol. 60, no. 21, pp. 5852–5861, 2005.
- [33] M. H. Habibi and M. Nasr-Esfahani, “Preparation, characterization and photocatalytic activity of a novel nanostructure composite film derived from nanopowder TiO_2 and sol-gel process using organic dispersant,” *Dyes and Pigments*, vol. 75, no. 3, pp. 714–722, 2007.
- [34] M. I. Cabrera, A. C. Negro, O. M. Alfano, and A. E. Cassano, “Photocatalytic reactions involving hydroxyl radical attack,” *Journal of Catalysis*, vol. 172, no. 2, pp. 380–390, 1997.
- [35] H. P. Klug and L. E. Alexander, *X-ray Diffraction Procedures*, chapter 9, John Wiley & Sons, New York, NY, USA, 1954.
- [36] D. C. Hague and M. J. Mayo, “The effect of crystallization and a phase transformation on the grain growth of nanocrystalline titania,” *Nanostructured Materials*, vol. 3, no. 1–6, pp. 61–67, 1993.
- [37] I. M. Arabatzis, S. Antonaraki, T. Stergiopoulos, et al., “Preparation, characterization and photocatalytic activity of nanocrystalline thin film TiO_2 catalysts towards 3,5-dichlorophenol degradation,” *Journal of Photochemistry and Photobiology A*, vol. 149, no. 1–3, pp. 237–245, 2002.